Polymer Journal, Vol. 11, No. 7, pp 565—574 (1979)

A Laser Scattering Photogoniometer

Yoshiyuki EINAGA, Tetsuo MITANI, Jyodo HASHIZUME, and Hiroshi FUJITA

Department of Polymer Science, Osaka University, Toyonaka, Osaka 560, Japan.

(Received December 27, 1978)

ABSTRACT: A computer-operated light scattering photogoniometer with a He–Ne laser (632.8 nm) as the light source was constructed, and the conditions for acquiring and processing data were investigated. The major features of the instrument are as follows. (1) Intensities of scattered light can be measured at a scattering angle as low as 5°. (2) A photon counting method is used for the measurement of scattering intensities. (3) Data acquisition and processing as well as the scanning of the photomultiplier over a specified range of scattering angles can be made with the aid of an on-line microcomputer. This instrument is tested with low-and high-molecular-weight polystyrene samples in benzene.

KEY WORDS Light Scattering Photogoniometer / He–Ne Laser / Microcomputer / Photon Counting / Rayleigh Ratio / Refractive Index Increment / Weight-Average Molecular Weight / Mean Square Radius of Gyration / Second Virial Coefficient / Polystyrene /

Light-scattering measurement of molecular weight and dimensions of a polymer in solution becomes increasingly difficult as these molecular parameters become larger. This difficulty can be circumvented by extending the measurement to a sufficiently small value of the scattering vector. The magnitude of the scattering vector is diminished either by lowering the scattering angle θ or by increasing the wavelength λ of incident light.[1-4] The recent advent of the laser has offered the possibility of satisfying these two requirements simultaneously. The high power and excellent spatial coherence of the laser as a light source make it possible to measure scattered light intensity at very small scattering angles. The use of the He–Ne laser, for example, permits measurement at a larger wavelength than when conducting experiments with a mercury vapor lamp as the light source. Keeping the test liquid away from the region where it may absorb light also enhances the effectiveness.

Such advantages motivated several groups of investigators[3-9] to construct various kinds of laser scattering instruments useful for the molecular characterization of giant polymers. In connection with a study on ultrahigh-molecular-weight samples of polystyrene, we have also designed and constructed a laser scattering photogoniometer with the cooperation of Union Giken Co., Osaka, Japan. The present paper describes the details and application of this instrument to "monodisperse" samples of polystyrene in benzene.

INSTRUMENTATION

Optical System

The arrangement of the optical parts in our instrument is depicted in Figure 1. A He–Ne laser (Nippon Electric Co., GLG2034) (1) operating in single transverse mode TEM_{00} with a 5 mW output is used as the light source. Vertically polarized laser light of 632.8 nm is in part reflected by a half-mirror (2) to a monitor. The remaining light travels through a converging lens (4), pinholes (5), a glass rod (6), and a light shield (7) and enters a test liquid placed in a highly polished cylindrical cell (8). The cell, made of Pyrex glass, is immersed in a refractive-index-matching solvent, xylene. The transmitted light is absorbved by a Rayleigh horn (14), while the scattered light is led to a photomultiplier (13) after passing through a series of slits (9). The incident and transmitted light are shielded by a pair of thin metal pipes (7). The receiver optical system consisting of the slit system, a periscope, the photomultiplier etc. is rigidly mounted on a lever arm, which can be rotated

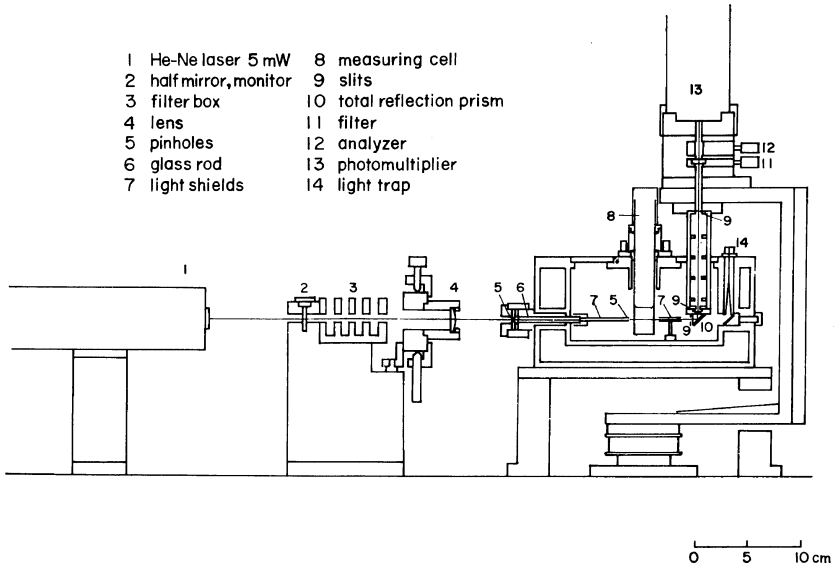

Figure 1. Arrangement of parts in the apparatus.

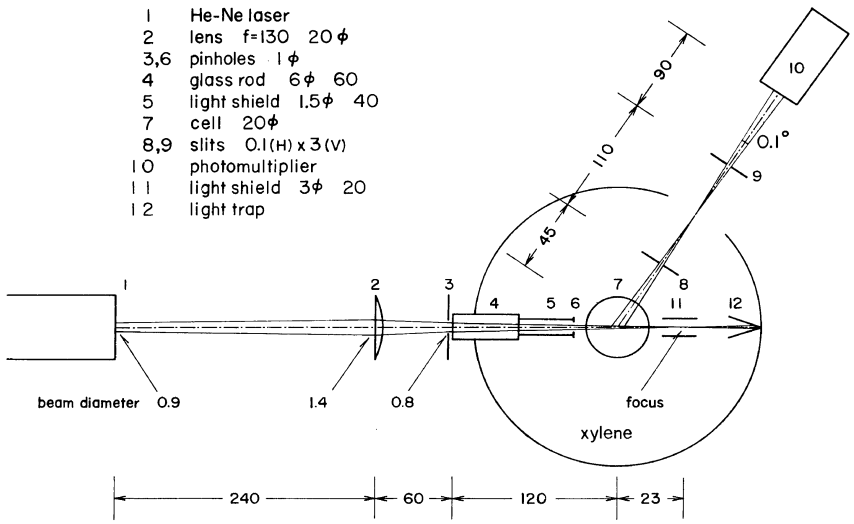

Figure 2. The optical system.

in a range of angles from 0 to 160°.

Spacings between the optical parts and the beam diameters are shown in Figure 2. According to the manufacturer's specifications, the beam diameter of our laser is about 0.9 mm at the exit of the source and spreads by an angle of about 1 milliradian. The divergent ray is converged by a lens (2) of focal length 130 mm, and lightly focused at about the midpoint of a light shield (11) in the absence of the scattering cell (7). The angular acceptance of the photomultiplier is estimated to be 0.1° from the spacing between two slits (8) and (9) and the diameters of their apertures.

Stray light generated as a result of multiple reflection on the surfaces of the half-mirror, the lens, the glass rod, and the exit window of the laser can be

eliminated by two aperture stops (3) and (6). Stray light which seriously disturbs measurements of scattered light intensity, particularly at low scattering angles, is produced in the bath. The axes of the glass rod and the incident beam must be completely matched. Otherwise, excessive rays are generated which travel back and forth between the end surfaces of the rod. It was very difficult to eliminate these rays by the aperture stop (6). Other causes of stray light in the bath are reflection at the interface between the cell wall and the test liquid or the bath liquid, and also the flareback of light reflected on the edge surface of the aperture stop (6). The view field of the photomultiplier is so limited by slits (8) and (9) that, even at an angle as low as 2°, the photomultiplier does not see the points at which the beam enters and leaves the cell. Nevertheless, it still catches the flares reflected from these points, although they can be diminished visually by rotating the cell adequately.

Bath and Measuring Cell

The structure of the bath is shown in Figure 1. The inner tank of diameter 137 mm is filled with a glass-refractive-index-matching liquid, xylene. The wall and the floor of the tank are blackened to minimize reflection of stray light. The tank is surrounded by a water jacket, which, in turn, is enclosed by a thickly nylon-coated wall. Water from a temperature-regulated reservoir (Julab, U-1) is circulated through the jacket and simultaneously thermostated xylene is pumped through the tank (see Figure 3). In this way, the bath can be thermostated to within ± 0.01°C.

The cells used for our routine measurements are 20 mm in outer diameter and 1.3 mm in thickness. Each measurement requires about 3 cm^3 of test liquid.

Electric System

Figure 3 shows a block diagram of the electric system used. A microcomputer system (Union Giken Co., System 70) operates the photogoniometer. Rotation of the receiver optical system, data acquisition, and data processing are all achieved by an on-line system according to the program written in Basic language or Assembler language. The lever arm mounting the receiver optical system is connected to a stepmotor which is driven stepwise with electric pulses generated by the computer; 100 pulses corresponds to a scanning angle of 1°. The position of zero angle is determined by rotating the lever arm until the transmitted light projects the sharpest spot on a screen placed in front of the photomultiplier. The computer measures scattering angles by counting the number of pulses delivered to the stepmotor.

The photomultiplier (Hamamatsu TV Co., R649) has an extended red response and is available for photon counting. It is operated by a high-voltage power supply. Generated photoelectric pulses are

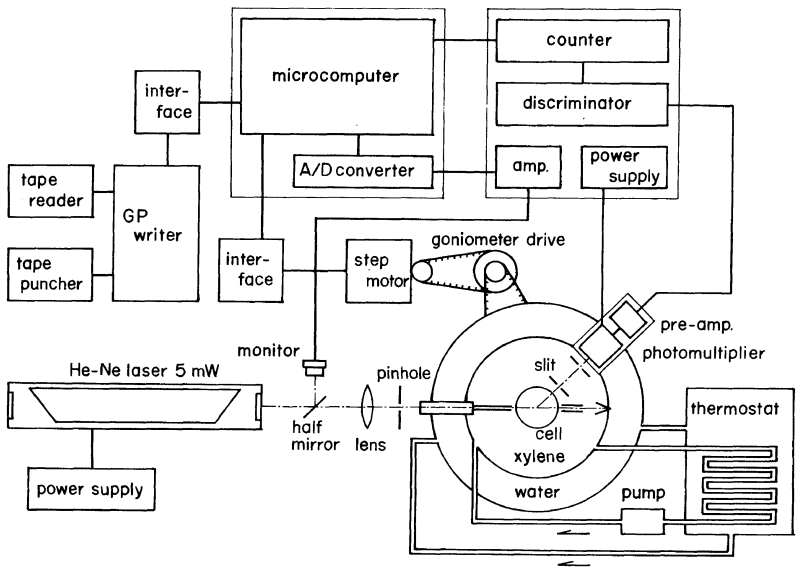

Figure 3. Block diagram of the electric system.

put into an amplifier (Hamamatsu TV Co., C716) and discriminated by a pulse-height discriminator (Hamamatsu TV Co., C1050-01) incorporated in the amplifier. Pulses higher than the prescribed discriminator level are squarized by a pulse shaper and delivered to a counter. The counted pulses include both dark and photoelectric ones. Since the probability densities of these pulses follow a Poisson distribution, the signal-to-noise ratio becomes larger as the pulse-counting interval increases.[9,10] The signal-to-noise ratio also depends on the discriminator level as well as the voltage supplied to the photomultiplier. These two voltages must be adjusted so as to optimize the photon counting.[11]

The stability of the laser source is monitored by allowing a small amount of the emitted laser light to be reflected on a silicon photocell (Hamamatsu TV Co., S780-8BK). The voltage from the photocell is amplified, sampled at discrete time intervals, and then digitized by an A/D converter. It remains constant to within $\pm 0.1\%$ for one hour and to within $\pm 0.5\%$ for one day when the laser source is adequately thermostated.

Both photon counts and digitized monitor-voltages are stored in the computer and delivered to a data processing. The input to and the output from the computer are provided by a GP writer.

CALIBRATION

Dead Time and Dark Pulses

The dead time of a photomultiplier restricts the range in which the intensity of light it receives is directly proportional to the number of pulses it generates.[12]. We checked this range of our photomultiplier by exposing it to fluorescence from a phosphor (see the next section). Photons of wavelengths longer than 690 nm were counted at various scattering angles with or without a neutral density filter, with a voltage of -1003 V applied to the photomultiplier and a voltage of 258 mV taken for the discriminator level. Figure 4 shows the counts for the fluorescence relative to those attenuated with the filter. They are almost constant at counting rates smaller than 1.5×10^5 counts s^{-1} and gradually decrease with an increase in counting rate. On the basis of this finding, all the light scattering measurements reported below were made, adopting the above-mentioned voltage conditions and photon counting rates below 1.5×10^5 counts s^{-1}.

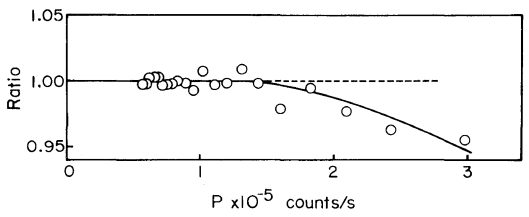

Figure 4. Effect of dead time on photon counting rate of the photomultiplier. See the text for details.

Since dark pulses disturb scattering intensity measurements, it is desirable to suppress these to a level as low as possible. In this regard, the photomultiplier we used was not very satisfactory. The dark pulse rate was about 30 counts s^{-1} at 15°C under the voltage conditions stated above; and it amounted to about one seventh of the 90° intensity of pure benzene at 25°C. However, the dark pulses fluctuated only from 290 to 330 in a series of data sampling when the sampling time was increased to 10 s. This fluctuation gives rise to a 2% variation in the 90° intensity of benzene at 25°C. In an actual calculation of scattering intensity, the average of the dark pulses before and after a data sampling was subtracted from the average of total counts including dark pulses.

Optical Alignment

Intensities of fluorescence from a phosphor were measured as a function of scattering angle. The phosphor was an aqueous solution of methylene blue with the concentration and PH of about 4×10^{-6} mol dm^{-3} and 3.4, respectively.[13] Since the

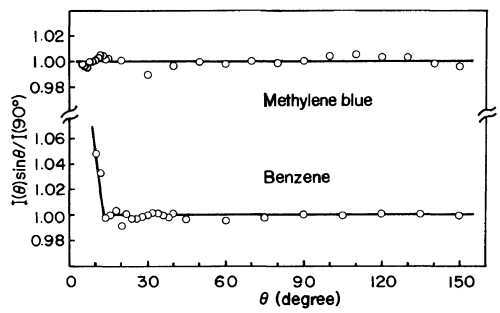

Figure 5. Angular dependence of reduced intensity $I(\theta)$ sin θ/I(90°C) of fluorescence from an aqueous solution of methylene blue and that of scattered light from benzene at 25°C.

viewing volume of a photomultiplier at an angle θ is approximated by the volume at 90° divided by sin θ, the photon count of fluorescence, $I(\theta)$, multiplied by sin θ should be independent of θ.[14] As expected, the measured values of $I(\theta)$ sin θ/I (90°) plotted against θ in Figure 5 scatter around a horizontal line in a range of angles from 5 to 150°, and their deviations from unity are smaller than 0.6% except for one point at 30° (1%). This result indicates a correct alignment of the optical system.

Stray Light

Intensities of light scattered from benzene at 25°C were measured at angles between 5 and 150° to estimate the amount of stray light. A spectroscopic grade benzene was rectified over sodium after it had been refluxed overnight and then centrifuged at 20000 rpm for 2 hours in a Sorval RC2-B centrifuge. The benzene thus prepared was directly pipetted into measuring cells. The cells and pipets were cleaned by rinsing them with distilled acetone in distillation columns.

The measurements were made for a combination of vertically polarized incident light and unpolarized scattered light. Scattered intensities $I(\theta)$ times sin θ relative to that at 90° are also plotted against θ in Figure 5. The values remain constant, with deviations of ±0.6%, for angles higher than 14°, suggesting that the photomultiplier caught no appreciable stray light in this range of angles. The intensity of stray light is 5% of the scattering intensity of benzene at 10° and 20% at 6° (not seen from the figure). We consider that this stray light was due mainly to reflection or scattering at points where the laser beam enters and leaves the cell. If so, its magnitude should depend on the spatial inhomogeneity of the cell galss, specks on the cell wall etc. and should be suppressable to some extent by rotating the cell until the flares at these points of the cell become minimum. We found that the upturn of $I(\theta)$ sin θ at low angles was practically the same for all the cells when the flares were minimized. Figure 6 shows the difference between the scattered light intensities (corrected for the scattering volume by multiplying sin θ) of benzene placed in two arbitrarily chosen cells. This difference vanishes within deviations of ±1% in the angular range 5—150°. This fact implies that for dilute solutions as treated in usual light scattering measurements, the excess scattering intensity over that of the solvent may not be disturbed by stray light if the scattering angle is not too low.

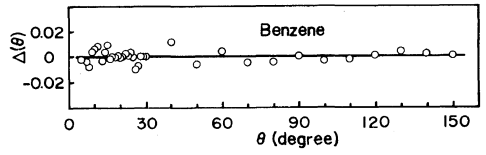

Figure 6. Differences between reduced scattering intensities $I(\theta)$ sin θ/I (90°) of benzene placed in different cells as a function of scattering angle.

Calculation of the Rayleigh Ratio

The Rayleigh ratio for the present instruments is defined by

$$R_\theta = \frac{i_\theta}{i_0}\frac{r^2 \sin\theta}{V_{90}}\left(\frac{n_s}{n_x}\right)^2$$

where i_0 is the irradiance of incident light, i_θ is that of scattered light at a distance r from a test liquid, V_{90} is the scattering volume at $\theta = 90°$, and n_s and n_x are the refractive indices of the test liquid and the bath liquid, xylene. The factors sin θ and $(n_s/n_x)^2$ are corrections of the viewing angle and refractive index for the volume seen by the photomultiplier.[9,14] The quantity (i_θ/i_0) is related to the computer reading for scattered light (I_θ) and that for monitored light (I_0) by

$$i_\theta/i_0 = A(I_\theta/I_0)$$

where A is a constant. Thus, the calibration constant C of the instument is given by

$$C = \frac{Ar^2}{V_{90}}\frac{1}{n_x^2}$$

The value of C was determined from the 90° scattering intensity of purified spectroscopic grade benzene at 25°C. As the Rayleigh ratio for a pair of vertically polarized incident and unpolarized scattered light of 632.8 nm, the value reported by Pike *et al.*,[15] $R_{90,Uv} = 11.84 \times 10^{-6}$ cm^{-1}, was assumed.

DATA ACQUISITION AND PROCESSING

In our apparatus, a microcomputer system controls all the data acquisition processes and treats acquired data by a software routine. The desired intensity of scattered light at a specified scattering angle is evaluated by a double averaging process. A

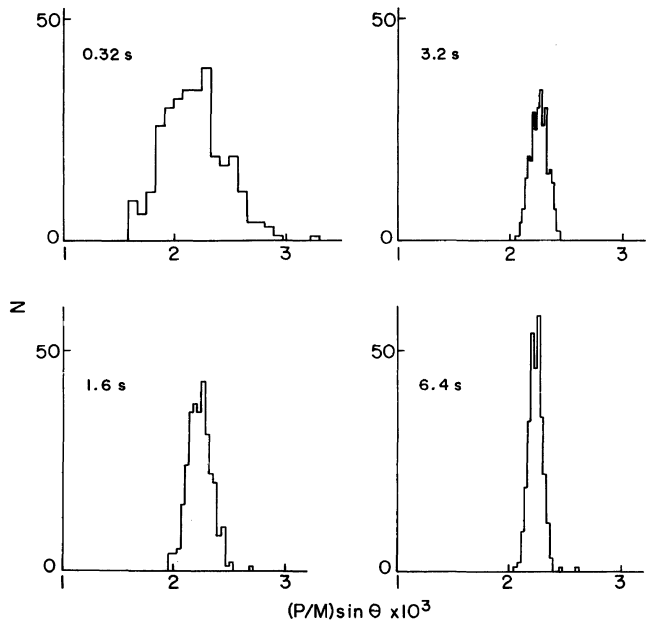

Figure 7. Histograms of photon counts obtained with different sampling times and at 30° for light scattered from purified benzene at 25°C.

range of angles, say, from 10 to 40°, is specified; up to 30 angles can be programmed in a specified range. At each angle, a set of photon count data is obtained by repeating data sampling with the sampling time held fixed, and the arithmetic mean is computed, discarding unusually deviated data if they appear. The mean value and the corresponding scattering angle are stored in the computer. Such data are accumulated by allowing the receiver optical system to go back and forth repeatedly over the specified range of angles (scans up to 40 can be programmed), and a set of the mean values obtained at each specified angle is again arithmetically averaged. In our computer system, the data sampling time can be set to any value larger than about 32 milliseconds with one millisecond as the unit and, at each stop of the receiver optical system, data up to 1000 samples can be accumulated. The rate of scanning is about one degree per second.

It is essential for routine work to find the data acquisition conditions which lead to an accurate determination of scattering intensity and yet are less time-consuming. After many trials, we found it relevant to set the sampling time between 1 and 10 s, to repeat data sampling 5 to 15 times at a specified angle, and to select the number of scans depending on the average intensity of scattered light in the specified range of angles.

Some basic data which led to the choice of these conditions are presented below. With the angle held fixed at 30° and purified benzene as the sample, photon counting was repeated 300 times for each of four sampling times from 0.32 to 6.4 s. The photon count distributions obtained are shown in Figure 7. The abscissa is the reduced photon count, *i.e.*, the measured count (including dark counts) P corrected for the intensity of the monitored light M and the scattering volume $(\sin\theta)^{-1}$. For each sampling time the range between the maximum and minimum of measured $(P/M)\sin\theta$ was divided into 20 intervals, and the number of samples with P falling in each of these intervals was taken as the ordinate value. The histogram becomes narrower as the sampling time is increased.

The narrowing of a histogram, in general, depends more directly on the magnitude of P rather than the length of the sampling time. For example, the maximum and minimum of P in a series of data sampling differed about 10% for a mean value $\bar{P}=1000$, 4% for $\bar{P}=4000$, and 2% for $\bar{P}=8000$—10000. Thus, if the sampling time is chosen so as to obtain a $\bar{P}$ value of the order of 10^4, we can determine

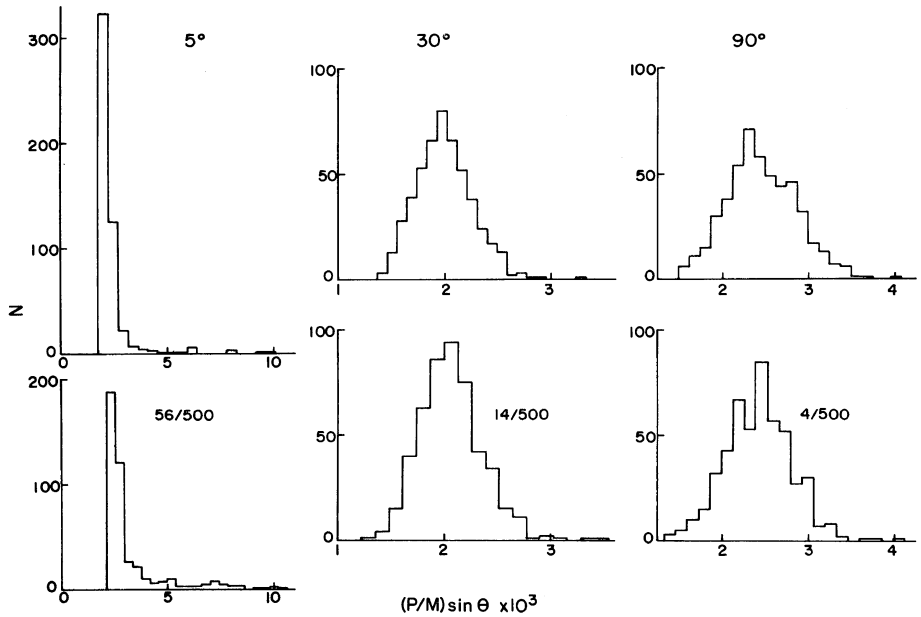

Figure 8. Histograms of photon counts at 5, 30, and 90° for scattered light from purified (upper row) and unpurified (lower row) benzene at 25°C.

a sufficiently accurate mean photon count with relatively few data samplings.

One of the most disturbing factors in light-scattering experiments is the presence of dust particles in test solutions. The histogram shown in Figure 7 should contain a contribution from dust particles, though we tried our best to clean the sample liquid. With the expectation that rapid data sampling may reveal effects of dust particles, a short sampling time of 0.32 s was chosen, and data sampling was repeated 500 times for both purified and unpurified benzene, at three scattering angles 5, 30, and 90°. The data for the purified benzene were treated as described above to obtain the histograms shown in the upper row of Figure 8. For the unpurified benzene, the samples with P above the upper bound of the corresponding histogram for the purified benzene were discarded, and the rest was analyzed in the same way as for the pure benzene. The resulting histograms are shown in the lower row of Figure 8. The number, say 14/500, in the figure means that 14 samples out of 500 were discarded in constructing a histogram. Thus, we see that more samples had to be discarded as the scattering angle was lowered.

The histogram for 30° of the purified benzene is approximately symmetric and has a small trail at a large abscissa value. Similar trails can also be seen in the histograms for 5 and 90° of the purified benzene. These small trails are probably due to dust particles or some other impurities, considering the fact that the number of samples in them increases as the scattering angle is lowered. However, their presence has only a negligible effect on the mean photon count unless the scattering angle is too low. Thus we conclude that if a test liquid is cleaned by the procedure described above, photon count data may be averaged with equal weight to calculate the desired scattering intensity.

It is seen from Figure 8 that if the data for large P values are discarded, the histograms for the unpurified benzene are not very different from those for the purified one. The mean values of $(P/M)\sin\theta$ for the unpurified benzene relative to that for the purified one calculated from these histograms for scattering angles 5, 30, and 90° are 1.12, 1.01, and 1.01, respectively, while the corresponding ratios computed without discarding any data are 2.82, 1.07, and 1.02. These values suggest that unfavorable scattering due to dust particles can be largely diminished by rapid data sampling and discarding data with large P by the cut-off procedure described

above.

APPLICATIONS

Our light scattering photogoniometer was tested with three "monodisperse" samples of polystyrene in benzene at 25°C. Toyo Soda's standard polystyrene F40 and F450 and a fraction F20-8 separated from Toyo Soda's standard polystyrene F20 were used. The solvent and solutions were cleaned according to the procedure described in a previous section.

The specific refractive-index increment $\partial n/\partial c$ for polystyrene in benzene at the wavelength $\lambda = 632.8$ nm has not been available in the literature up to now. We estimated this value by plotting the literature values $0.1094\,\mathrm{cm^3\,g^{-1}}$ at $\lambda = 435.8$ nm and $0.1062\,\mathrm{cm^3\,g^{-1}}$ at $\lambda = 546.2$ nm against λ^{-2} and extrapolating the straight line fitting them to $\lambda = 632.8$ nm.[14,16] The extrapolated value was $0.1047\,\mathrm{cm^3\,g^{-1}}$.

Figures 9 through 12 depict the light scattering envelopes for sample F40, plotted in accordance with Berry's proposal.[17] Figure 9 shows the concentration dependence of $(Kc/R_\theta)^{1/2}$ at fixed scattering angles between 10 and 150°. Here, c is the polymer mass concentration, R_θ is the Rayleigh ratio at a scattering angle θ, and K is the familiar optical factor.[14] The data points at each angle are closely fitted by a straight line and can be extrapolated to a zero polymer concentration with high precision. The angular dependence of $(Kc/R_\theta)^{1/2}$ at fixed concentrations, shown in Figure 10, exhibits a similar feature; a set of data points at each concentration follows a straight line and permits an accurate extrapolation to zero angle. This graph omits most of the data obtained at lower scattering angles in order to show the trend of $(Kc/R_\theta)^{1/2}$ in a wide range of angles. The data at scattering angles between 10 and 45° appear enlarged in Figure 11. Here, the straight lines indicated are the reproduction of those in Figure 10. It is seen that the data points are somewhat more scattered than those in Figure 10. This is attributed to the fact that the sampling time used to obtain these low-angle data was 1 s, while for the wide-angle data, the time was increased to 10 s.

The values of $(Kc/R_\theta)^{1/2}$ at zero concentration extrapolated from Figure 9 and those at zero angle from Figure 10 are plotted together in Figure 12, where the square of the scattering vector, instead of $\sin^2(\theta/2)$, is used to compare data at different

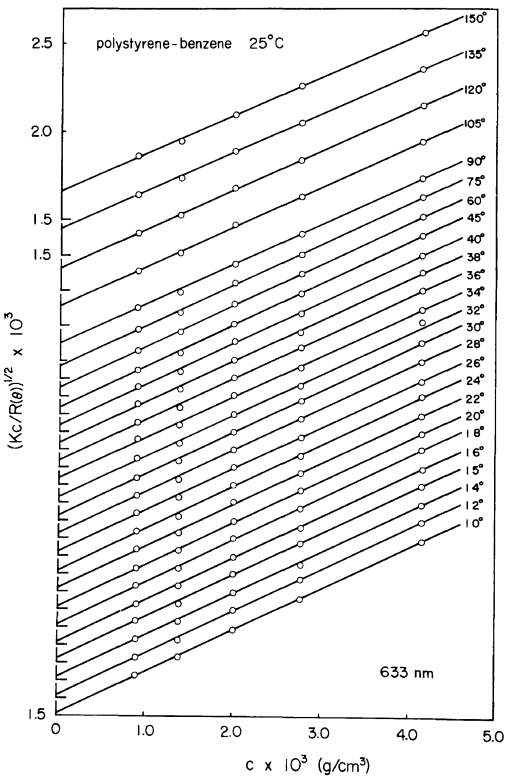

Figure 9. Reciprocal square-root of reduced scattering intensities at fixed angles as a function of polymer concentration c for sample F40 in benzene at 25°C.

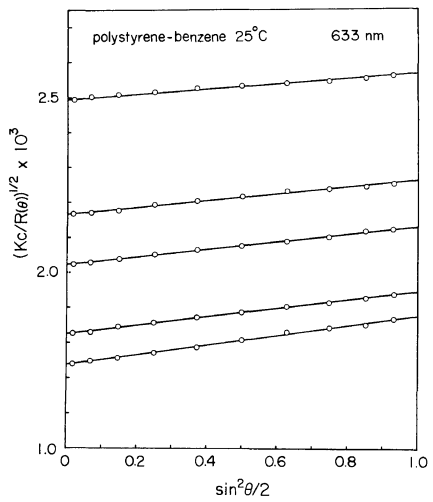

Figure 10. Angular dependence of reciprocal square-root of reduced scattering intensities at concentrations, 4.1472×10^{-3}, 2.7648×10^{-3}, 2.0109×10^{-3}, 1.3824×10^{-3}, and $0.8965 \times 10^{-3}\,\mathrm{g\,cm^{-3}}$, from top to bottom, for sample F40 in benzene at 25°C.

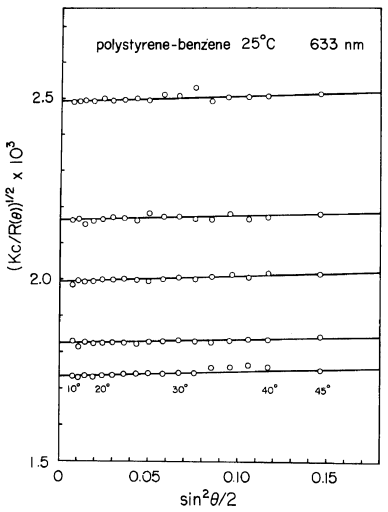

Figure 11. Enlarged plots of reciprocal square-roots of reduced scattering intensities at angles smaller than 45° against $\sin^2\theta/2$ for the same solutions as in Figure 10. The straight lines indicated are the same as those in Figure 10.

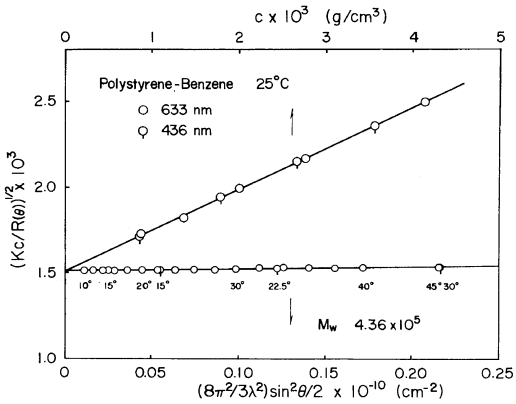

Figure 12. Reciprocal square-roots of reduced scattering intensities extrapolated to zero polymer concentration or to zero scattering angle for sample F40 in benzene at 25°C. Unpiped and piped circles represent the data obtained at 632.8 nm by the present photogoniometer and those at 435.8 nm by a Fica 50 instrument, respectively.

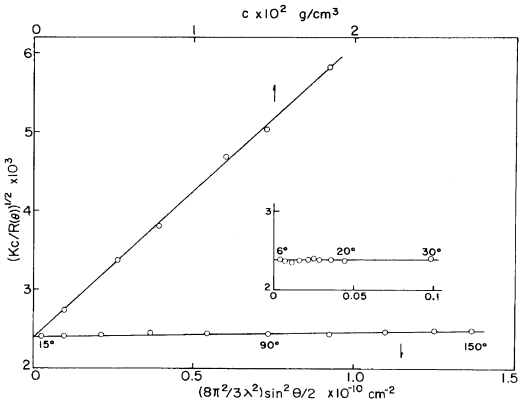

Figure 13. Reciprocal square-root of reduced scattering intensities extrapolated to zero concentration or to zero scattering angle for sample F20-8 in benzene at 25°C. The insert shows the angular dependence of the data at angles smaller than 30°. The values of $\bar{M}_w$, $\langle S^2\rangle^{1/2}$, and A_2 from these plots are $(1.74\pm0.05)\times10^5$, 16 ± 4 nm, and $(4.45\pm0.05)\times10^{-4}$ mol cm³ g⁻², respectively.

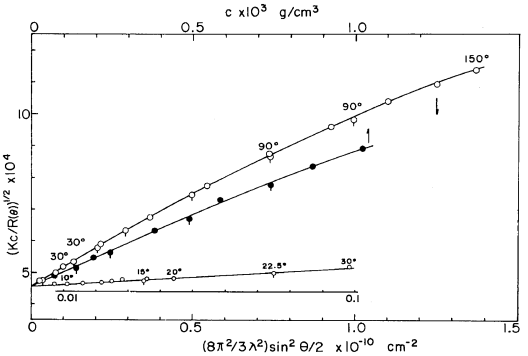

Figure 14. Reciprocal square-root of reduced scattering intensities extrapolated to zero concentration (open circles) or to zero scattering angle (closed circles) for sample F450 in benzene at 25°C. Unpiped and piped circles represent the data obtained at 632.8 nm by the present photogoniometer and those at 546.2 nm by a Fica 50 instrument, respectively. Smaller circles show the data at angles below 30°. The plots give $(4.83\pm0.1)\times10^6$, 116 ± 2 nm, and $(2.10\pm0.03)\times10^{-4}$ mol cm³ g⁻², respectively, for $\bar{M}_w$, $\langle S^2\rangle^{1/2}$, and A_2.

wavelengths. The piped data points were obtained at $\lambda=435.8$ nm by use of a conventional Fica 50 photogoniometer. The good agreement of the piped and nonpiped points deserves appreciation. The weight-average molecular weight $\bar{M}_w$, the root mean square radius of gyration $\langle S^2\rangle^{1/2}$, and the second virial coefficient A_2 evaluated from the lines in Figure 12 are $4.3_6\times10^5$, 26 nm, and $3.5_9\times10^{-4}$ mol cm³ g⁻², respectively.

The values of $(Kc/R_\theta)^{1/2}$ for sample F20-8 extrapolated to zero angle or to zero polymer concentration are shown in Figure 13, and the corresponding data for sample F450 are presented in Figure 14. Again, the piped points in the lattter figure show the data obtained at 546.2 nm by use of the Fica 50 instrument. The value of $\bar{M}_w$, $\langle S^2\rangle^{1/2}$, and A_2 estimated

from these graphs are indicated in the respective figure captions. The slope of the line for infinite-dilution values of $(Kc/R_\theta)^{1/2}$ for sample F20-8 is so small that it permits determination of $\langle S^2 \rangle^{1/2}$ only approximately. Our laser-scattering photogoniometer is of little use for such small polymer dimensions. The scattering envelope for sample F450 at infinite dilution exhibits an appreciable downward curvature, as can be expected for this very high-molecular-weight polymer in good solvents. Its intercept and initial slope could be determined only approximately if reliable data were not available at scattering angles below 20°, which is the lowest angle for reliable measurements by a conventional light-scattering instrument. The infinite-dilution data on sample F450 for angles smaller than 30° obtained by the present apparatus and Fica 50 instrument are plotted in the lower part of Figure 14. They are accurately fitted by a straight line and permit determination of $\bar{M}_w$ and $\langle S^2 \rangle^{1/2}$ with precision.

The original aim of this study has been to construct a light-scattering apparatus useful for characterizing polymer samples of ultrahigh-molecular-weight, say, higher than 10^7. In fact, with the present apparatus, we have succeeded in determining the molecular weight and radius of gyration of a polystyrene sample of $\bar{M}_w$ close to 6×10^7, and have reported these data in a recent paper.[18]

Acknowledgements. The construction of this instrument was made possible by a grant-in-aid for scientific research from the Ministry of Education. The technical cooperation of Union Giken Co., Osaka, Japan, is gratefully acknowledged. Thanks are rendered to Dr. M. Fukuda of Toyo Soda Co., Japan, for supplying the polystyrene samples used for our measurements.

REFERENCES

1. J. A. Harpst, A. I. Krasna, and B. H. Zimm, *Biopolymers*, **6**, 585 (1968).
2. H. Utiyama, N. Sugi, M. Kurata, and M. Tamura, *Bull. Inst. Chem. Res., Kyoto Univ.*, **46**, 198 (1968).
3. Von A. Burmeister and G. Meyerhoff, *Ber. Bunsenges. Phys. Chem.*, **78**, 1366 (1974).
4. V. J. Morric, H. J. Coles, and B. R. Jennings, *Nature*, **249**, 240 (1974).
5. J. A. Finnigan, D. J. Jacobs, and J. C. Marsden, *J. Colloid Interface Sci.*, **37**, 102 (1971).
6. A. M. Wims and M. E. Myers, Jr., *J. Colloid Interface Sci.*, **39**, 447 (1972).
7. W. Kaye, *Anal. Chem.*, **45**, 221A (1973).
8. D. Thiel, B. Chu, A. Stein, and G. Allen, *J. Chem. Phys.*, **62**, 3689 (1975).
9. D. Jolly and H. Eisenberg, *Biopolymers*, **15**, 61 (1976).
10. C. J. Oliver and E. R. Pike, *Br. J. Appl. Phys.*, **1**, 1459 (1968).
11. R. Foord, R. Jones, C. J. Oliver, and E. R. Pike, *Appl. Opt.*, **8**, 1975 (1969).
12. F. A. Johnson, R. Jones, T. P. Mclean, and E. R. Pike, *Phys. Rev. Lett.*, **16**, 589 (1966).
13. E. Robinowitch and L. F. Epstein, *J. Am. Chem. Soc.*, **63**, 69 (1941).
14. M. B. Huglin, "Light Scattering from Polymer Solutions," Academic Press, London and New York, N.Y., 1972.
15. E. R. Pike, W. R. M. Pomeroy, and J. M. Vaughan, *J. Chem. Phys.*, **62**, 3188 (1975).
16. O. Bodmann, *Makromol. Chem.*, **122**, 196 (1969).
17. G. C. Berry, *J. Chem. Phys.*, **44**, 4550 (1966).
18. Y. Miyaki, Y. Einaga, and H. Fujita, *Macromolecules*, **11**, 1180 (1978).